

Tolerance analysis of a 4x4 MMI-based 90° optical hybrid for 100G coherent receivers

J. S. Fandiño, P. Muñoz and J. Capmany
Optical and Quantum Communications Group.
ITEAM Research Institute.

Universitat Politècnica de València, c/ Camino de Vera s/n, 46020 Valencia (Spain).
E-mail: jasanfan@upvnet.upv.es

Abstract—A tolerance analysis of a 4x4-MMI working as a 90° optical hybrid in InP technology is presented. Results predict up to 25 nm bandwidth. 50 nm are expected for width tolerances below $\pm 0.1 \mu\text{m}$.

I. INTRODUCTION

Revived interest in coherent optical communications has recently spurred much research in 90° optical hybrids, which have become a fundamental component of coherent receivers. Although several structures have been proposed [1], robustness and tolerance to manufacturing defects make 4x4 MultiMode Interference couplers (4x4 MMI) perfect candidates for fully integrated, high performance 90° optical hybrids. Devices with imbalance below 0.5 dB and phase errors lower than 5° across the whole C band have been already demonstrated using 4 μm SOI technology [2]. Common Mode Rejection Ratios (CMRRs) below 20 dBc for both I and Q channels and phase errors below 7° were also demonstrated in InP over the whole C-band within a temperature range from -5°C to 75°C [3].

However, ever-increasing data traffic will likely require the use of even more complex modulation formats. Tighter restrictions in optical front-end PICs will put a limit to manufacturing tolerances, so as to meet imbalance and phase specifications. In this work, a study on the impact of manufacturing tolerances in the performance of a 4x4 MMI, designed using InP generic integration technology, is presented. Several

physical parameters are considered: waveguide's width, core's thickness, core's refractive index, length, and wavelength. Parameters impact is derived in terms of metrics established in the Optical Internetworking Forum (OIF) standard draft for 100G integrated intradyne coherent receivers, such as the CMRR and phase errors for both I & Q channels.

II. SIMULATION PROCEDURE

An overview of the device structure and waveguide cross-section is shown in Fig. 1. Waveguides consists of two layers: InGaAsP as core ($n = 3.258 @ \lambda = 1.55 \mu\text{m}$) over an InP substrate ($n = 3.169 @ \lambda = 1.55 \mu\text{m}$). They are defined by etching down 600 nm from the top of the core. Firstly, a nominal 90° hybrid was designed using commercial software tools to serve as a reference for the tolerance analysis.

Secondly, technology specific manufacturing tolerances were taken into account. These include absolute maximum variations in waveguide's width ($\pm 0.1 \mu\text{m}$) due to lithography and etching steps, as well as refractive index (± 0.004) and thickness ($\pm 0.05 \mu\text{m}$) due to epitaxial growth. Wavelength was also considered to assess operation bandwidth ($\pm 50 \text{ nm}$). Simulation values ([range]@step) are: MMI length=[848,860]@3 μm , $n_{\text{core}}=[3.250,3.266]@0.004$, MMI width=[19.8,20.2]@0.1 μm and core thickness=[0.9,1.1]@0.05 μm . Wavelength interval is [1.5,1.6]@0.25 μm , along with two additional points at 1.5375 and 1.625 μm . Multi-sweep runs were performed, and optical transmission relations between input (2 4) and output (1 2 3 4) ports (Fig. 1) were calculated.

Finally, CMRRs and phases were derived from photodetected currents, and compared with worst-case values given by the OIF standard draft: CMRR Signal to I & Q $\leq -20 \text{ dBc}$, CMRR LO to I & Q $\leq -12 \text{ dBc}$ as well as phase error between I and Q channels $\leq \pm 5^\circ$. CMRRs are related to cancellation of common mode noise (e.g. RIN), while phase errors result in loss of orthogonality and crosstalk between I and Q channels.

III. RESULTS AND DISCUSSION

Our tolerance analysis expands in a 5th dimensional space. A versatile visualization technique called *dimensional stacking* was employed to represent results and gain insight into relationships among parameters [4]. This concept is summarized in Fig. 2 (left). For every wavelength, a matrix is plotted

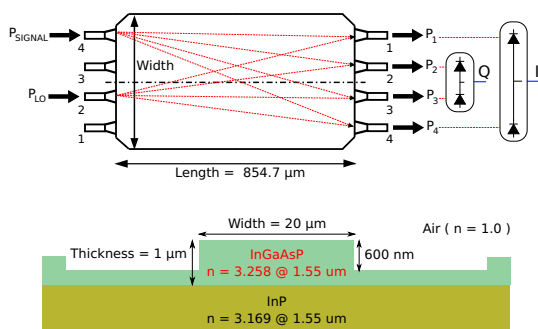


Fig. 1: Top and cross-section view. Nominal device values are shown.

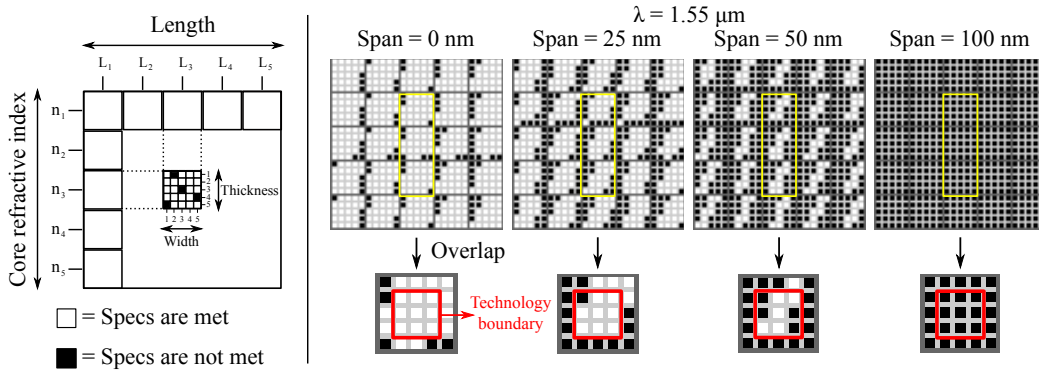


Fig. 2: Left: Dimensional stacking plot diagram, showing distribution of input parameters. Right: Simulation results for different spans.

which contains 5x5 submatrices of 5x5 pixels. Each of these groups contains those simulations where width (horizontal) and thickness (vertical) are varied, while length and refractive index remain fixed. Parameter values increase from left to right and from top to bottom, i.e., pixels in the center of each matrix represent nominal design values. A pixel is coloured white when all specifications are met (both CMRR and phase), and black otherwise.

The final result can be seen also in Fig. 2 (right), where matrices for different wavelength spans are shown. These were formed by overlapping all those matrices whose simulation wavelength falls within a given span around the nominal wavelength (e.g. the 25nm span matrix is formed by overlapping matrices at 1.5375, 1.55 and 1.5625 μm). From these pictures, some interesting conclusions can be drawn. Firstly, it is easily observed that pixel patterns inside each group remain almost unchanged when moving in the vertical direction. This means that waveguide’s core refractive index has no significant effect on device performance, which is consistent with basic MMI theory. A change in core refractive index will affect effective indexes of all propagation modes. Since optimum length depends on the difference between them, common changes are cancelled out. Secondly, device is also shown to be highly tolerant to length variations, which span a 15 μm range. This is also consistent with MMI theory and with the fact that CMRRs only measure similarity between output powers, so total insertion losses are not taken into account.

Further processing of this binary data can also be used to estimate operation bandwidth for a given set of manufacturing tolerances. Reversely, it can be employed to define maximum manufacturing deviations to achieve certain design goals (such as bandwidth). In this work, the former approach is considered. We provide values for HHI’s InP generic integration technology, but the concept can be applied to any other technology. In general, length manufacturing deviations approach those related to the width ($\pm 0.1 \mu\text{m}$ in this particular case), which are much lower than those required to cause an impact in device performance. Thus, length can be reasonably assumed to be constant. Afterwards, groups related to technology maximum deviations in n_{core} are overlapped in the vertical direction (Fig. 2, yellow line). The resultant 2D plots shows which combina-

tions of width and thickness match specifications across the given span, assuming that deviations in refractive index can not be controlled. By considering only those contained within the boundary specified by technology (Fig. 2, red line), an approximate 25 nm bandwidth is expected, which is consistent with previous experimental results [3]. Fig. 2 also shows that an accuracy better than $\pm 0.1 \mu\text{m}$ would be required to achieve operation bandwidth up to 50 nm, regardless of variations in waveguide’s thickness.

IV. CONCLUSIONS

A tolerance analysis of a 90° optical hybrid based on a 4x4 MMI monolithically integrated in an InP generic integration technology has been performed. CMRRs and phase relations have been analyzed. Simulations show that these specifications can be met, at least, over a 25 nm range for the chosen InP generic integration technology, in good agreement with previous experimental results. Further bandwidth (up to 50 nm) is expected to require accuracy in MMI’s width better than $\pm 0.1 \mu\text{m}$.

ACKNOWLEDGEMENTS

The authors acknowledge financial support from Spanish MICINN Project TEC2010-21337, acronym ATOMIC. J.S. Fandiño acknowledges financial support through grant FPU-2010 (ref: AP2010-1595). The authors are also grateful to the EuroPIC consortium (FP7 funded programme NMP 228839-2) for access to the design manual and design toolkit of the generic InP fab.

REFERENCES

- [1] M. Seimetz and C.-M. Weinert, “Options, feasibility, and availability of 2x4 90 hybrids for coherent optical systems,” *Lightwave Technology, Journal of*, vol. 24, pp. 1317–1322, march 2006.
- [2] L. Zimmermann, K. Voigt, G. Winzer, K. Petermann, and C. Weinert, “C-band optical 90 hybrids based on silicon-on-insulator 4x4 waveguide couplers,” *Photonics Technology Letters, IEEE*, vol. 21, pp. 143–145, feb.1, 2009.
- [3] H.-G. Bach, A. Mattis, C. Leonhardt, R. Kunkel, D. Schmidt, M. Schell, and A. Umbach, “Monolithic 90 hybrid with balanced pin photodiodes for 100 gbit/s pm-qpsk receiver applications,” in *OFC 2009*, pp. 1–3, march 2009.
- [4] J. LeBlanc, M. Ward, and N. Wittels, “Exploring n-dimensional databases,” in *Visualization, 1990. Visualization '90., Proceedings of the First IEEE Conference on*, pp. 230–237, oct 1990.